

# Strangeness Production Process $pp \rightarrow nK^+\Sigma^+$ within Resonance Model

Xu Cao<sup>1,3</sup>, Xi-Guo Lee<sup>1,2\*</sup>, and Qing-Wu Wang<sup>1,3</sup>

1. *Institute of Modern Physics, Chinese Academy of Sciences,  
P.O. Box 31, Lanzhou 730000, P.R.China*

2. *Center of Theoretical Nuclear Physics,  
National Laboratory of Heavy Ion Collisions, Lanzhou 730000, P.R.China*

3. *Graduate School, Chinese Academy of Sciences, Beijing 100049, P.R.China*

## Abstract

We explore production mechanism and final state interaction in the  $pp \rightarrow nK^+\Sigma^+$  channel based on the inconsistent experimental data published respectively by COSY-11 and COSY-ANKE. The scattering parameter  $a > 0$  for  $n\Sigma^+$  interaction is favored by large near-threshold cross section within a nonrelativistic parametrization investigation, and a strong  $n\Sigma^+$  interaction comparable to  $pp$  interaction is also indicated. Based on this analysis we calculate the contribution from resonance  $\Delta^*(1920)$  through  $\pi^+$  exchange within resonance model, and the numerical result suggests a rather small near-threshold total cross section, which is consistent with the COSY-ANKE data. With an additional sub-threshold resonance  $\Delta^*(1620)$ , the model gives a much better description to the rather large near-threshold total cross section published by COSY-11.

PACS numbers: 13.75.Cs; 14.20.Gk; 13.30.Eg; 13.75.Ev

---

\* Email: xgl@impcas.ac.cn

## I. INTRODUCTION

Strangeness production process in nucleon-nucleon collisions has attracted considerable theoretical interest since high precision data have been published in the past few years[1, 2, 3, 4, 5, 6, 7, 8]. This field is fascinating for several reasons. First of all, strangeness production in nucleon-nucleon collisions is an elementary process, and their cross sections are an fundamental input into transport model calculations of the strangeness production in heavy ion collisions. Furthermore, strangeness production process may provide information on the strange components of the nucleon and deepen our knowledge on the internal structure of nucleon[22]. Finally, for the short life time of hyperons, it is difficult to accumulate a large set of scattering events and obtain accurate scattering parameters. Final state interaction (FSI) in strangeness production can supply us with assistant information on the KN and YN interaction.

A series of theoretical models[9, 10, 11, 12, 13] have given excellent description to the observed energy dependence of the total cross section for the strangeness production process  $pp \rightarrow pK^+\Lambda$  and  $pp \rightarrow pK^+\Sigma^0$ . Some of these models[11, 12, 14] also give a reasonable explanation to the energy dependence of the ratio  $R = \sigma(pp \rightarrow pK^+\Lambda)/\sigma(pp \rightarrow pK^+\Sigma^0)$ . Compared to the detailed experimental and theoretical investigation in these two channels, there is only limited data on the total cross section for  $pp \rightarrow nK^+\Sigma^+$ . A recent COSY-ANKE data[26] indicates a rather small near-threshold total cross section, which is much smaller than previous COSY-11 data[25]. For the large error bar of these experimental data, any definite conclusion cannot be surely drawn at present, and it must be checked in future experiments.

On the other hand, as a good isospin-3/2 filter without complication caused by  $N^*$  contribution,  $pp \rightarrow nK^+\Sigma^+$  is an excellent channel for the investigation of  $\Delta^*$  resonance[17]. It is necessary to deepen our theoretical understanding to the controversial experimental data. In this paper, we use a resonance model and its nonrelativistic parametrization to explore the energy dependence of the total cross section of the  $pp \rightarrow nK^+\Sigma^+$ . In section II we introduce the Feynman diagrams and the effective Lagrangian approach within resonance model. In section III we present a exploration to the near threshold region within a nonrelativistic parametrization and give a set of FSI parameters. In section IV, we give the numerical results and explore their implications, especially in the near threshold region.

Section V provides a summary.

## II. RESONANCE MODEL AND EFFECTIVE LAGRANGIAN APPROACH

The treatment of the elementary processes  $NN \rightarrow NYK$  is tree level at the hadronic level in the resonance model[9], as illustrated in Figure 1. All interference terms between different amplitudes are neglected because the relative phases of these amplitudes can not be fixed by the scarce experimental data. Mesons exchanged are restricted to those observed in the decay channels of the adopted resonances, and kaon exchange is not included in the calculation. Thus, all values of the coupling constants are fixed by the experimental decay ratios, and the only adjustable parameters are cut-off parameters in the form factors. In this model, only  $\Delta^*(1920)$  through  $\pi^+$  exchange contributes to the  $pp \rightarrow nK^+\Sigma^+$  channel above the production threshold. The relevant meson-nucleon-nucleon(MNN) and resonance-nucleon(hyperon)-meson effective Lagrangians for evaluating the Feynman diagrams in Fig. 1 are:

$$L_{\pi NN} = -ig_{\pi NN}\bar{N}\gamma_5\vec{\tau} \cdot \vec{\pi}N, \quad (1)$$

$$L_{\Delta(1920)N\pi} = \frac{g_{\Delta(1920)N\pi}}{m_\pi}\bar{N}\Delta_\mu\vec{\tau} \cdot \partial^\mu\vec{\pi} + h.c., \quad (2)$$

$$L_{\Delta(1920)\Sigma K} = \frac{g_{\Delta(1920)\Sigma K}}{m_K}\Delta_\mu\vec{I} \cdot \vec{\Sigma}\partial^\mu K + h.c., \quad (3)$$

where  $N, \Delta_\mu, K$  and  $\vec{\pi}$  are the Rarita-Schwinger spin wave function of the nucleon, the resonance, the kaon and the pion respectively,  $\vec{\tau}$  the Pauli matrices,  $\vec{I}$  the spin-3/2 matrices and  $g_{\pi NN}^2/4\pi = 14.4$ . The effective Lagrangians for the resonance  $N^*$  please refer to [9, 15, 16, 17, 18].

For the propagators of  $\pi$  meson and the spin-3/2  $\Delta^*(1920)$  resonance, the usual Rarita-Schwinger propagators are used:

$$G_\pi(k_\pi) = \frac{i}{k_\pi^2 - m_\pi^2}, \quad (4)$$

$$G_R^{\mu\nu}(p_R) = \frac{\gamma \cdot p + m_R}{p_R^2 - m_R^2 + im_R\Gamma_R} \left[ g_{\mu\nu} - \frac{1}{3}\gamma_\mu\gamma_\nu - \frac{1}{3m_R}(\gamma_\mu p_\nu - \gamma_\nu p_\mu) - \frac{2}{3m_R^2}p_\mu p_\nu \right], \quad (5)$$

TABLE I: Relevant  $\Delta^*(1920)$  parameters

	Width	Channel	Branching ratio	Adopted value	$g^2/4\pi$
$\Delta^*(1920)$	200MeV	$N\pi$	0.05-0.20	0.125	0.0034
		$\Sigma K$	0.01-0.03	0.021	0.0292

with  $k_\pi$  and  $p_R$  being the four momentum of  $\pi$  meson and  $\Delta^*(1920)$  resonance respectively,  $m_\pi$  and  $m_R$  the corresponding masses. The relations between the branching ratios and the coupling constants then can be calculated using the relevant Lagrangians. Take  $\Delta^*(1920) \rightarrow N\pi$  as an example:

$$\Gamma_{\Delta(1920)N\pi} = \frac{g_{\Delta(1920)N\pi}^2}{m_\pi^2} \frac{(m_N + E_N)(P_N^{cm})^3}{12\pi M_{\Delta(1920)}}, \quad (6)$$

$$P_N^{cm} = \frac{\lambda^{1/2}(m_{\Delta(1920)}^2, m_N^2, m_\pi^2)}{2M_{\Delta(1920)}}, \quad E_N = \sqrt{(P_N^{cm})^2 + m_N^2}, \quad (7)$$

here  $\lambda(x, y, z) = x^2 + y^2 + z^2 - 2xy - 2yz - 2zx$ . Then the coupling constants can be determined through the empirical branching ratios. Values related to  $\Delta^*(1920)$  are summarized in Table I[9, 17].

The resulting  $\pi NN$  and  $\Delta(1920)N\pi$  vertexes are multiplied by form factors which dampen out high values of the exchanged momentum:

$$F_M(\vec{q}) = \frac{\Lambda_M^2 - m_M^2}{\Lambda_M^2 - q_M^2}, \quad (8)$$

with  $\Lambda_M$ ,  $q_M$  and  $m_M$  being the cut-off parameter, four-momentum and mass of the exchanged meson.  $\Lambda_\pi = 1.3\text{GeV}$  as the widely used value[9, 15, 17]. The form factor of the  $\Delta(1920)\Sigma K$  vertex is 1.

As to  $pp \rightarrow nK^+\Sigma^+$  channel, if the only contribution comes from resonance  $\Delta^*(1920)$  through  $\pi^+$  exchange, the corresponding amplitude can be obtained straightforwardly by applying the Feynman rules to Fig. 1:

$$M = \frac{g_{\Delta(1920)\Sigma K}}{m_K} \bar{u}_{(p_\Sigma)}^{(S_\Sigma)} p_K^\mu G_{\Delta(1920)}^{\mu\nu} p_{\Delta(1920)}^\nu \frac{g_{\Delta(1920)N\pi}}{m_\pi} u_{(p_1)}^{(S_1)} p_\pi^\nu G_\pi(p_\pi) \bar{u}_{(p_n)}^{(S_n)} \sqrt{2} g_{\pi NN} \gamma_5 u_{(p_2)}^{(S_2)}$$

$$+ (\text{exchange term with } p_1 \leftrightarrow p_2), \quad (9)$$

Final state interaction influences the near-threshold behavior significantly. It has been experimentally and theoretically verified that  $p\Lambda$  FSI is essential to the  $pp \rightarrow pK^+\Lambda$  process. Similarly, here only  $n\Sigma^+$  interaction is considered with Watson-Migdal factorization[19], and  $nK^+$  interaction will not be taken into account for its weakness[8]:

$$A = MT_{n\Sigma}, \quad (10)$$

where  $T_{n\Sigma}$  is the enhancement factor describing the  $n\Sigma^+$  final state interaction and goes to unity in the limit of no FSI, as expected by the physical picture. Similar to the  $p\Lambda$  FSI in the  $pp \rightarrow pK^+\Lambda$  channel, we assume that  $T_{n\Sigma}$  can be taken to be Jost function[20]:

$$T_{n\Sigma} = \frac{q + i\beta}{q - i\alpha}, \quad (11)$$

$$q = \frac{\lambda^{1/2}(s, m_\Sigma^2, m_n^2)}{2\sqrt{s}}, \quad s = (\varepsilon + m_n + m_K + m_\Sigma)^2, \quad (12)$$

with  $\varepsilon$  being the excess energy. The related scattering length and effective range are:

$$a = \frac{\alpha + \beta}{\alpha\beta}, \quad r = \frac{2}{\alpha + \beta}, \quad (13)$$

Then the total cross section can be calculated by:

$$\sigma_{tot} = \frac{m_p^2}{4F} \int |\mathcal{M}|^2 \delta^4(p_1 + p_2 - p_n - p_K - p_\Sigma) \frac{m_n d^3 p_n}{E_n} \frac{d^3 p_K}{2E_K} \frac{m_\Sigma d^3 p_\Sigma}{E_\Sigma}, \quad (14)$$

with the flux factor  $F = (2\pi)^5 \sqrt{(p_1 \cdot p_2)^2 - m_p^4}$ .  $|\mathcal{M}|^2$  is the square of the invariant scattering amplitude, averaged over the initial spins and summed over the final spins. The integration over the phase space can be performed by Monte Carlo program.

For the lack of the  $n\Sigma^+$  scattering data, a set of data are employed referring to the  $p\Lambda$  interaction[21] in the Ref.[17]'s calculation:

$$\alpha = -75.0 \text{ MeV}, \quad \beta = 200.0 \text{ MeV}, \quad (15)$$

The corresponding scattering length and effective range are:

$$a = -1.6 \text{ fm}, \quad r = 3.2 \text{ fm}, \quad (16)$$

Next we will concentrate on the relation between FSI and the near-threshold total cross section, and try to find some clues on the  $n\Sigma^+$  interaction. As a matter fact, we fix scattering length and effective range with a nonrelativistic parametrization, assuming no possible quasi-bound or molecular state.

### III. NONRELATIVISTIC PARAMETRIZATION AND FSI

It is generally agreed that the energy variation of the total cross section for the  $pp \rightarrow pK^+\Lambda$  and  $pp \rightarrow pK^+\Sigma^0$  is fixed mainly by the  $\varepsilon^2$  factor coming from phase space, modified by the FSI in the near-threshold region:

$$\sigma_{tot} \propto \varepsilon^2 \times FSI, \quad (17)$$

If  $|M|^2$  depend smoothly on the excess energy, Eq.(14) can be parameterized as[21, 23]:

$$\sigma_{tot} = \frac{\sqrt{m_N m_K m_\Sigma}}{2^7 \pi^2 (m_N + m_K + m_\Sigma)^{3/2}} \frac{\varepsilon^2}{\lambda^{1/2}(s, m_N^2, m_N^2)} |M|^2 \kappa, \quad (18)$$

$$\kappa = 1 + \frac{4\beta^2 - 4\alpha^2}{(-\alpha + \sqrt{\alpha^2 + 2\mu\varepsilon})^2}, \quad (19)$$

where  $\kappa$ , the FSI factor, was firstly put forward by G. Fäldt and C. Wilkin[28]. At sufficiently large  $\varepsilon$ ,  $\kappa \rightarrow 1$  and FSI can be isolated. It is noted that the nonrelativistic phase space factor is used in the above equation, and this is a good approximation up to excess energies of  $\varepsilon \simeq 1\text{GeV}$ . In order to give some clues to the  $n\Sigma^+$  interaction, the physical mechanism of strangeness production will not be concerned, and  $|M|^2$  is parameterized as  $|M|^2 \propto e^{-const.\varepsilon}$ . Similar parametrization[21] has give an excellent description to the energy dependence of the total cross section for the  $pp \rightarrow pK^+\Lambda$ ,  $pp \rightarrow pK^+\Sigma^0$  and the ratio  $R = \sigma(pp \rightarrow pK^+\Lambda)/\sigma(pp \rightarrow pK^+\Sigma^0)$ .

If parameters in FSI factor are employed to be the same with Eq.(16), and  $|M|^2 = 18.9e^{-1.3\varepsilon} \cdot 10^6 \mu b$  ( $\varepsilon$  in GeV), the total cross section for  $pp \rightarrow nK^+\Sigma^+$  as a function of excess energy can be exhibited by the solid curve in Fig. 2. It gives a reasonable description to the total cross section in high energies and underestimates the COSY-11 data, which is consistent with the numerical calculation below(see Fig.3). This verifies the applicability of the parametrization Eq.(18).

If  $n\Sigma^+$  FSI is negligible ( $\kappa = 1$ ) and  $|M|^2 = 21.2e^{-1.3\varepsilon} \cdot 10^6 \mu b$ , the result is dashed curve in Fig. 2. It still overestimates COSY-ANKE data by a factor of about 3. As a matter of fact, the pure phase space behavior is favored by so small near-threshold total cross section, as indicated by the dotted curve with  $\kappa = 1$  and  $|M|^2 = 4.7 \cdot 10^6 \mu b$ . This means that  $n\Sigma^+$  FSI is negligible, similar to the  $p\Sigma^0$  FSI in  $pp \rightarrow pK^+\Sigma^0$ , but the scattering amplitude is more weakly dependent on the excess energy. If the near-threshold total cross section is really as small as COSY-ANKE data[26], the nearly constant scattering amplitude is the extraordinary character for  $pp \rightarrow nK^+\Sigma^+$  channel.

However, in order to reproduce COSY-11 data, totally different parameters should be adopted:

$$|M|^2 = 20e^{-1.7\varepsilon} \cdot 10^6 \mu b, \quad (20)$$

$$\alpha = 30MeV, \quad \beta = 360MeV, \quad (21)$$

The result is the dash-dotted curve in Fig. 2. The corresponding scattering length  $a = 7.1fm > 0$  (with  $r = 1.0fm$ ) is contrary to the values used in the Ref.[17]'s calculation (Eq.(16)) and implies an even stronger  $n\Sigma^+$  interaction. It is worth noting that the scattering parameters of  $pp$  interaction are  $a = -7.8fm$  and  $r = 2.8fm$ . In the next section we will give a comparison between these two sets of  $n\Sigma^+$  FSI parameters, and show that a better reproduce to the large near-threshold total cross section is achieved with Eq.(21).

#### IV. NUMERICAL RESULTS AND IMPLICATION

The contribution from resonance  $\Delta^*(1920)$  through  $\pi^+$  exchange with FSI parameters in Eq.(16) is shown as the dotted curve in Fig. 3. Note that the resonance  $\Delta^*(1920)$  can be treated as an effective resonance which represents all contributions of six resonances ( $\Delta^*(1900), \Delta^*(1905), \Delta^*(1910), \Delta^*(1920), \Delta^*(1930)$ , and  $\Delta^*(1940)$ ) and the coupling constants relevant to  $\Delta^*(1920)$  are scaled multiplying by a factor[27]. The numerical result (the dashed curve in Fig. 3) reproduces the data in high energies reasonably well but underestimates COSY-11 data by a factor of orders, as pointed out in above section. It has been suggested[17] that the inclusion of a ignored sub-threshold resonance  $\Delta^*(1620)1/2^-$

(both  $\rho^+$  and  $\pi^+$  exchange are included), together with a strong  $n\Sigma^+$  FSI in Eq.(16), would achieve much better agreement, as illustrated by the solid curve in Fig. 3. Unfortunately, it still underpredicts two near-threshold data points. It is argued[17] that improvement can be achieved by inclusion of the interference term between  $\rho^+$  and  $\pi^+$  exchange. However, this kind of interference term is very small as demonstrated in another channel  $pp \rightarrow pK^+\Lambda$ [16], and it definitely can not provide any interpretation to this relatively large discrepancy.

The numerical result showed by the dashed curve in Fig. 3 agrees COSY-ANKE data, which was obtained at a little higher energy and shows a rather small total cross section in near-threshold region, as indicated by a closed star in Fig. 3.

The numerical results with the FSI parameters in Eq.(21) are given in Fig.4. The contribution from resonance  $\Delta^*(1920)$  through  $\pi^+$  exchange is not affected much by the alteration of the FSI parameters, and still gives a small near-threshold total cross section. This indicates that the contribution from resonance  $\Delta^*(1920)$  is not sensitive to the magnitude of the  $n\Sigma^+$  interaction, and we would be not able to distill any valuable information about the  $n\Sigma^+$  interaction. However, the contribution from resonance  $\Delta^*(1620)$  gives an even larger near-threshold cross section, and the resulting curve reproduces all previous published data reasonably, as illustrated by the solid curve in Fig. 4. This strongly suggests a rather strong  $n\Sigma^+$  interaction if the near-threshold cross section is as large as COSY-11 data[25]. We would like to stress that this is incompatible to the known YN scattering data. Besides, the  $p\Sigma^0$  interaction is found to be weak in  $pp \rightarrow pK^+\Sigma^0$  channel, and the naive speculation is that the  $n\Sigma^+$  interaction should be weak, too. One may further expect that the energy dependence of the  $pp \rightarrow nK^+\Sigma^+$  is approximately the same with that of  $pp \rightarrow pK^+\Sigma^0$ [29]. Anyway, due to the scarcity and uncertainty of those experimental data, the conclusion that these data imply a highly anomaly near-threshold behavior can not be definitely drawn yet. Based on these numerical result, we may also conclude that contribution from  $\Delta^*(1620)$  is indispensable for a good reproduce to the large near-threshold total cross section, which has been discussed deeply in the Ref.[17].

## V. SUMMARY

We presented the confusion caused by the existing data for  $pp \rightarrow nK^+\Sigma^+$  channel. The numerical result and parametrization analysis reveal a large discrepancy between two sets of



near-threshold data, which means totally different  $n\Sigma^+$  interaction. The theoretical results presented in other works[21] also indicated that the total cross section data alone cannot distinguish different production mechanisms. In order to clarify the confusion that if there was a highly abnormal near-threshold behavior in  $pp \rightarrow nK^+\Sigma^+$  channel, it is necessary to accumulate a data set with high accuracy and large statistics. Further measurements are being planned in COSY-ANKE[29]. Besides, a significant improvement is to be expected through the installation of Cooling Storage Ring (CSR) in Lanzhou, China, which is designed for the study of heavy-ion collisions. It can provide  $1 \sim 2.8\text{GeV}$  proton beam and perform accurate measurement to differential observables and invariant mass spectrum. In Ref.[21] the authors proposed a scheme to study the role of the FSI by analyzing Dalitz plot distribution, and experiment performed by COSY-TOF Collaboration[8] verified their prediction. Similar analysis may also clarify the confusion in  $pp \rightarrow nK^+\Sigma^+$  channel. So CSR 's data may offer an opportunity to explore the reaction mechanism for the strange production process in nucleon-nucleon collisions. Only then it is possible to achieve an acceptable confidence level for the near-threshold behavior and the dynamical mechanism in the  $pp \rightarrow nK^+\Sigma^+$  channel.

### Acknowledgments

We would like to thank J. J. Xie and B. S. Zou for fruitful discussions and program code. We also thank Colin Wilkin for a careful reading of the draft and valuable comments. This work was supported by the CAS Knowledge Innovation Project (No.KJCX3-SYW-N2,No.KJCX2-SW-N16) and Science Foundation of China (10435080, 10575123,10710172).

- 
- [1] J. T. Balewski et. al., *Phys, Lett. B* **388**, 859 (1996); **420**, 211 (1998).
  - [2] H. Brand et. al., *Phys, Lett. B* **420**, 217 (1998).
  - [3] S. Sewerin et. al., *Phys. Rev. Lett.* **83**, 682 (1999).
  - [4] P. Moskal et. al., *J. Phys. G* **28**, 1777 (2002).
  - [5] M. Wolke et. al., *Nucl. Phys. A* **721**, 683 (2003).
  - [6] P. Kowina et. al., *Eur. Phys. J. A* **18**, 351 (2003); **22**, 293 (2004).
  - [7] T. Rozek et. al., *Int. J. Mod. Phys. A* **20**, 680 (2005).

- [8] S. Abd El-Samad et. al., *Phys. Lett. B* **632**, 27 (2006).
- [9] K. Tsushima, A. Sibirtsev, A.W. Thomas, *Phys. Rev. C* **59**, 369 (1999).
- [10] G. Fäldt, C. Wilkin, *Z. Phys. A* **357**, 241 (1997).
- [11] R. Shyam, G. Penner, U. Mosel, *Phys. Rev. C* **63**, 022202 (2001); R. Shyam, *Phys. Rev. C* **60**, 055213 (1999)
- [12] A. Gasparian et. al., *Phys. Lett. B* **480**, 273 (2000).
- [13] L.-M. Laget, *Phys. Lett. B* **259**, 24 (1991); *Nucl. Phys. A* **691**, 11 (2001)
- [14] A. Sibirtsev, K. Tsushima, W. Cassing, A.W. Thomas, *nucl-th/0004022*.
- [15] R. Machleidt, K. Holinde, Ch. Elster, *Phys. Rep.* **149**, 1 (1987).
- [16] B. C. Liu, B. S. Zou, *Phys. Rev. Lett.* **96**, 042002 (2006); *Commun. Theor. Phys.* **46**, 501 (2006).
- [17] J.J. Xie, B.S. Zou, *Phys. Lett. B* **649**, 405 (2007).
- [18] J. J. Xie, B. S. Zou, H.C.Chiang, *arXiv:0705.3950*.
- [19] K. Watson, *Phys.Rev.* **88**, 1163 (1952); A.B. Migdal, *Sov. Phys. JETP* **1**, 2(1955).
- [20] M. Goldberger, K.M. Watson, *Collision Theory Willey, New York.* (1964).
- [21] A. Sibirtsev et. al., *Eur. Phys. J. A* **29**, 263(2006); **27**, 269(2006).
- [22] B. S. Zou, D. O. Riska, *Phys. Rev. Lett* **95**, 072001 (2005).
- [23] A. Sibirtsev et. al., *Eur. Phys. J. A* **32**, 229 (2007).
- [24] A. Baldini, V. Flamino, W. G. Moorhead and D. R. O. Morrison, *Landolt-Bornstein, Numerical Data and Functional Relationships in Science an Technology, vol.12, ed. by H.Schopper, Springer-Verlag(1988), Total Cross Sections of High Energy Particles..*
- [25] T. Rozek et. al., *Phys. Lett. B* **643**, 251 (2006).
- [26] Yu. Valdau et. al., *Phys. Lett. B* **652**, 245 (2007).
- [27] K. Tsushima, S. W. Huang, and Amand Faessler, *Phys. Lett. B* **337**, 245 (2005); *J. Phys. G* **21**, 33 (1995).
- [28] G. Fäldt, C. Wilkin, *Phys. Lett. B* **354**, 20 (1995); *Physica. Scripta* **56**, 566 (1997).
- [29] C. Wilkin, private commucation.

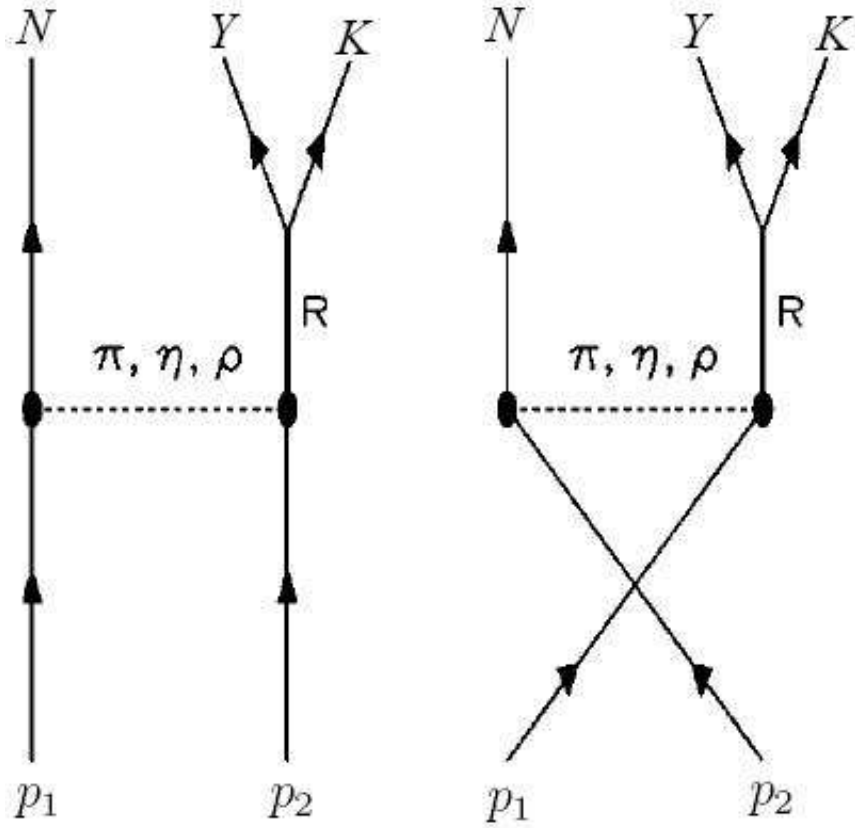


FIG. 1: Feynman diagrams in the resonance model.  $N$ ,  $Y$  and  $K$  stand for, respectively, the nucleon, the hyperon and the kaon.  $R$  is the resonance.

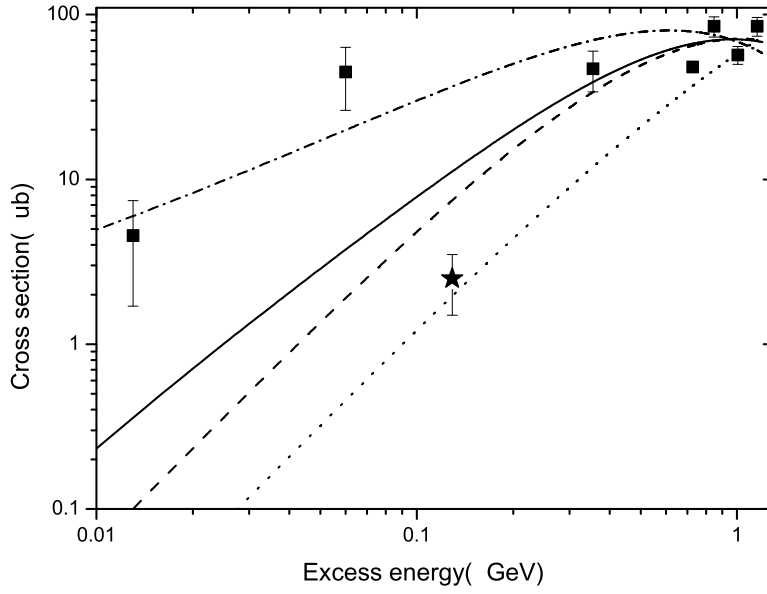


FIG. 2: Total cross section for  $pp \rightarrow nK^+\Sigma^+$  as a function of excess energy. The relevant parameters used for the curves refer to the text. Data are taken from Ref.[24], COSY-11[25](closed square) and COSY-ANKE[26] (closed star).

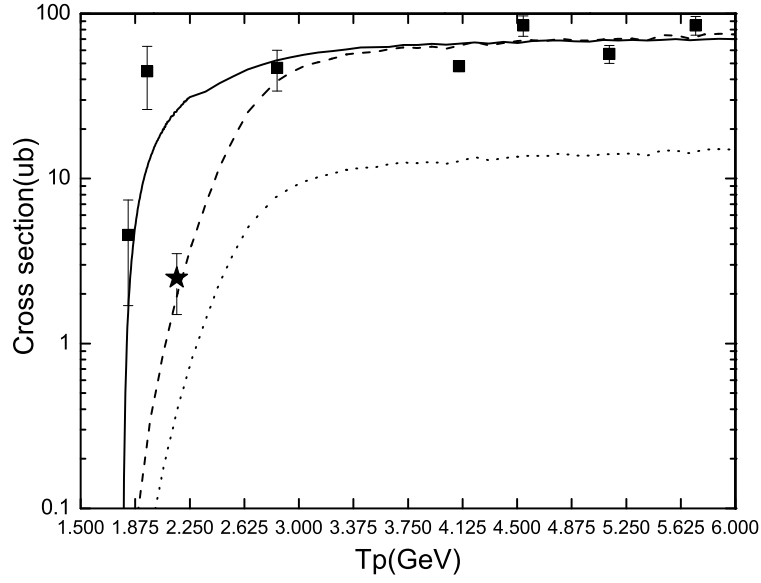


FIG. 3: Variation of the total cross section with the kinetic energy of the proton beam ( $T_p$ ). Dotted curve: contribution from resonance  $\Delta^*(1920)$  through  $\pi^+$  exchange. Dashed curve: contribution from resonance  $\Delta^*(1920)$  scaled multiplying by a factor 5. Solid curve: numerical result in the Ref.[17]. Data are the same as in Figure 2.

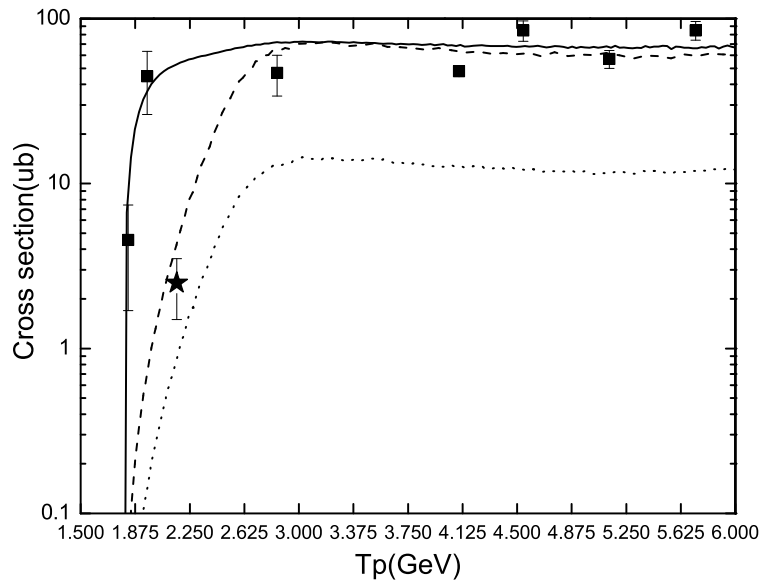


FIG. 4: Same as in Fig. 3, but with the FSI parameters in Eq.(21). Data are the same as in Figure 2.